Resonant-Cavity-Enhanced Single-Photon Avalanche Diodes on Reflecting Silicon Substrates

Massimo Ghioni, *Member, IEEE*, Giacomo Armellini, Piera Maccagnani, Ivan Rech, Matthew K. Emsley, and M. Selim Ünlü, *Fellow, IEEE*

***Abstract*—In this letter, we report the first resonant-cavity-enhanced single-photon avalanche diode (RCE SPAD) fabricated on a reflecting silicon-on-insulator (SOI) substrate. The substrate incorporates a two-period distributed Bragg reflector fabricated using a commercially available double-SOI process. The RCE SPAD detectors have peak photon detection efficiencies ranging from 42% at 780 nm to 34% at 850 nm and time resolution of 35-ps full-width at half-maximum. Typical dark count rates of 450, 3500, and 100 000 c/s were measured at room temperature with RCE SPADs having, respectively 8-, 20-, and 50-μm diameter.**

***Index Terms*—Photon counting, resonant cavity enhanced (RCE), silicon-on-insulator (SOI), single-photon avalanche diode (SPAD), time-correlated single-photon counting (TCSPC).**

I. Introduction

SILICON single-photon avalanche diodes (SPADs) have gained wide acceptance for single-photon counting (SPC) and time-correlated SPC (TCSPC) applications over the visible spectral range up to 1-μm wavelength. In recent years, photon detection modules employing low-voltage SPAD detectors with diameters up to 100 μm have become commercially available from various manufacturers. Such detectors are fabricated in planar technology on epitaxial silicon substrates and offer the typical advantages of solid state devices (miniaturization, ruggedness, low voltage, low power, low cost, etc.) along with excellent photon timing resolution <35-ps full-width at half-maximum (FWHM) and a high photon detection efficiency (PDE) in the visible range ($\sim$50% at 550 nm) [1]. The PDE of planar SPADs typically varies from 25% to 12% in the near-infrared (NIR) range from 700 to 850 nm, being much higher than that of photomultiplier tubes equipped with standard S20 or S25 photocathodes. Nevertheless, a better PDE performance in the NIR range would be highly desirable in various fields, as for instance high bit-rate, short-wavelength quantum key distribution [2], and in-vivo molecular imaging for life sciences applications [3].

The most straightforward way of achieving higher PDE in SPAD detectors is to increase the depletion region thickness. However, the need of ensuring a high electric field strength (above the critical value for breakdown) over a thick depletion layer leads to high operating voltage, causing substantial power dissipation and self-heating problems. Furthermore, a thick depletion region would make the photon-assisted propagation mechanism to dominate the jitter of the avalanche current leading-edge, resulting in worse photon timing performance [4]. Therefore, it is desirable to enhance the PDE without increasing the absorption layer thickness.

A Fabry–Pérot cavity can be exploited to enhance the optical field inside the SPAD detector at resonant wavelengths [5]. Such a resonant cavity can be formed using a buried reflector and the air–semiconductor top interface [6]. This approach enables higher PDE at the same depletion region thickness, thus avoiding adverse effects on photon timing resolution and power dissipation.

In this letter, we report the first planar SPAD device grown atop a highly reflective two-period silicon-on-insulator (SOI) substrate. We demonstrate that these resonant-cavity-enhanced (RCE) SPADs provide a substantial PDE improvement in the NIR, while keeping excellent photon timing resolution and low operating voltage.

II. Device Fabrication

RCE SPAD fabrication started from 4-in reflecting silicon wafers having an epitaxy ready single crystalline surface. These wafers incorporate a two-period distributed Bragg reflector (DBR) fabricated using a commercially available double-SOI process. The thickness of the DBR layers (437 nm for the SiO_2 layers and 174 nm for the Si layers) was specifically tuned to achieve a reflectance in excess of 90% around 850 nm [6]. On top of these reflecting wafers, double epitaxial SPADs with active area diameter of 8, 20, and 50 μm were fabricated using the planar process described in [7]. Fig. 1 shows a schematic cross section of the RCE SPAD detector. The active n + p junction is built in the upper low-doped p-epilayer. The buried p+ epilayer provides a low-resistance path to the side ohmic contact. The total thickness of the epilayers is about 5 μm. A boron implantation in the central part of the n + p junction defines the high electric field region, that is, the active area of the detector. Deep, highly doped n+ regions provide electrical isolation between adjacent SPADs and act as gettering sites for transition metals. The silicon substrate acts as a control gate

Manuscript received November 12, 2007. This work was supported by the European Commission FP6, Information Society Technologies (NANOSPAD Project IST-NMP2-016610 and SECOQC Project IST-2002-506813).

M. Ghioni, G. Armellini, and I. Rech are with Politecnico di Milano, Dipartimento di Elettronica e Informazione, 20133 Milan, Italy (e-mail:ghioni@elet.polimi.it; armellini@elet.polimi.it; rech@elet.polimi.it).

P. Maccagnani is with IMM-CNR, 40129 Bologna, Italy (e-mail: maccagnani@bo.imm.cnr.it).

M. K. Emsley is with Analog Devices Inc., Wilmington, MA 01887 USA (e-mail: Matthew.Emsley@analog.com).

M. S. Ünlü is with the Department of Electrical and Computer Engineering, Boston University, Boston, MA 02215 USA (e-mail:selim@bu.edu).

Color versions of one or more of the figures in this letter are available online at http://ieeexplore.ieee.org.

Digital Object Identifier 10.1109/LPT.2008.916926

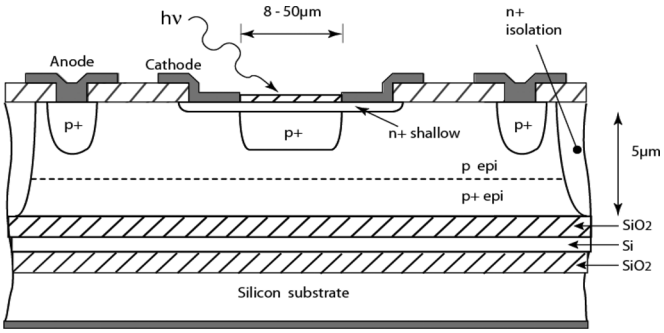

Fig. 1. Schematic cross section of the RCE SPAD detector.

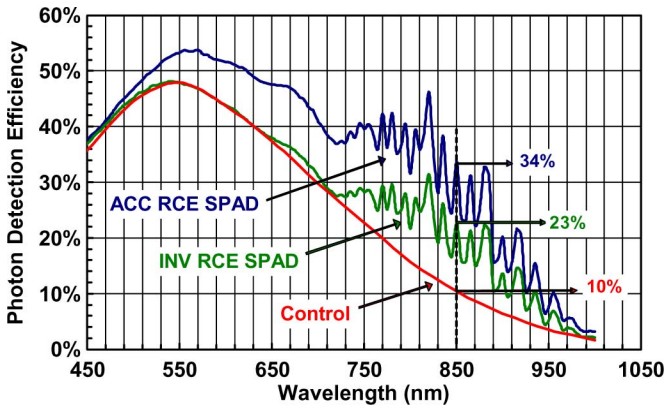

Fig. 2. PDE as a function of wavelength for control SPAD detector and RCE SPAD detector with INV or ACC layer formed at the Si–SiO_2 buried interface.

to induce an inversion (INV) or accumulation (ACC) layer at the buried Si–SiO_2 interface. Al contacts were deposited by sputtering, and patterned photolithographically. The active area of SPAD detectors was coated with a single 100-nm-thick SiO_2 layer to prevent reliability problems. The reflectivity of the coated surface is about half of that of bare silicon–air surface at 850 nm (14% instead of 32%), resulting in a lower finesse of the resonant cavity, that is, a lower enhancement of the PDE.

"Control" SPAD detectors made on conventional n-type substrates were fabricated in the same batch for comparison purposes.

III. Experimental Results and Discussion

Preliminary tests on RCE SPAD detectors were performed at room temperature. An average breakdown voltage of 32.5 V with a standard deviation of 0.6 V was measured for SPADs with 50-μm diameter randomly distributed on the wafer.

Dark count rate (DCR) was measured by operating SPAD detectors at 5-V excess bias voltage with an external active quenching circuit (AQC). A hold-off time of 300 ns was enforced by the AQC such that afterpulsing effects are reduced to a negligible level. The typical DCR is 450, 3500, and 100 000 c/s for SPADs having respectively 8-, 20-, and 50-μm active area diameter. The DCR of control SPADs is about one order of magnitude lower, showing that the defectivity of double-SOI substrates is higher. PDE measurements were performed using a dedicated setup including a halogen light source, monochromator, integrating sphere, and a reference silicon photodetector. The PDE of RCE SPAD detectors was measured in two different conditions, namely with an INV layer or an ACC layer formed at the buried Si–SiO_2 interface. These two conditions were easily obtained by applying a suitable voltage between substrate and anode contacts, that is, about -10 V for accumulation and $+10$ V for inversion. Fig. 2 shows the PDE of control and RCE SPADs as a function of wavelength, measured at 5-V excess bias voltage. As expected, no resonance peaks are observable in RCE SPADs up to 650 nm, since either most of the incident photons are absorbed before reaching the buried mirror or the buried mirror itself has a low reflectivity [6]. In contrast, resonant enhancement of PDE occurs between 750 and 950 nm where the buried mirror has its maximum reflectivity and the absorption lengths are greater than 10 μm. A remarkable PDE of 34% was measured at 850 nm for RCE SPADs with ACC layer. The PDE reduces to

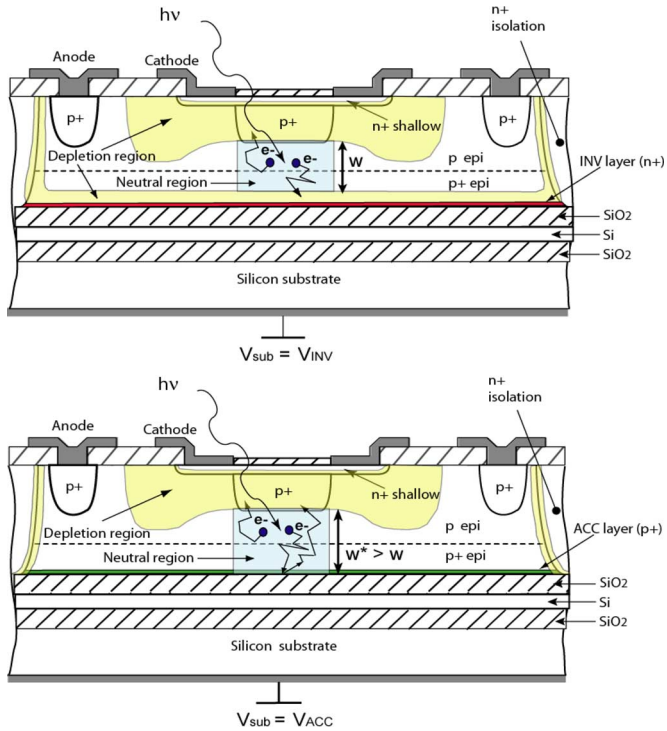

Fig. 3. Cross section of the RCE SPAD detector showing the effect of the INV layer (top) and of the ACC layer (bottom) on diffusing minority electrons.

23% at the same wavelength by inducing an INV layer at the buried Si–SiO_2 interface. This figure, however, still favorably compares with the PDE of control SPAD detectors (10%).

The noticeable difference between the PDE of RCE SPADs with INV and ACC layers is due to minority carriers photogenerated in the neutral region beneath the active junction (see Fig. 3). If an INV layer is formed, the reverse biased n-isolation/p-epilayer junction is extended all over the buried Si–SiO_2 acting as a buried p-n junction. Minority carriers diffusing toward the buried reflector are captured by the reverse-biased buried junction, giving no photon signal. A similar loss of minority carriers happens in conventional SPAD detectors, where the p-type epitaxial layers are grown over a n-type substrate.

In contrast, if an ACC layer is formed, there is no buried junction and the neutral region extends all the way down to the buried

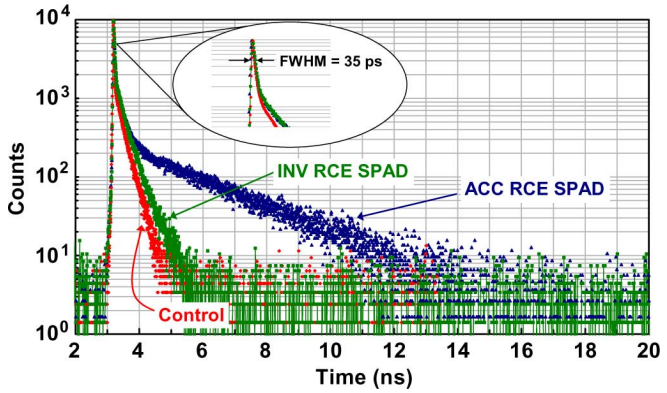

Fig. 4. Time response of RCE and control SPAD detectors to a laser diode emitting 15-ps optical pulses at 820 nm. Tested SPADs have an active area diameter of 50 μm and are operated at 5-V excess bias voltage.

Si–SiO_2 interface. Minority carriers diffusing toward the buried reflector may be backscattered and eventually captured by the active junction, where they may trigger an avalanche pulse. In practice, there is almost no loss of minority carriers photogenerated in the neutral region, resulting in a higher PDE. It must be noted that this mechanism enhances the PDE at all wavelengths for which the optical absorption in the neutral layer is not negligible (i.e., $\lambda > 500$ nm), independently of the optical reflectivity of the buried mirror.

The inherent wavelength selectivity of RCE SPADs might be a drawback in applications where the incoming light has a narrow spectrum, since strict control of the epilayer thickness would be required to accurately set the resonance wavelength. To avoid the need for complex spectral tuning procedures [6] and yet still benefit from the RCE structure, one can coat the top surface of the detector with an antireflection coating which will result in a "two-pass" detector where the light enters the photodetector and reflects off the buried mirror, thus doubling the effective absorption width.

Time resolution measurements were performed in a conventional TCSPC setup by using an ultrafast laser diode (Antel MPL-820 laser module) emitting 15-ps FWHM optical pulses at 820-nm wavelength. Fig. 4 shows the time response of 50-μm -diameter RCE and control SPADs. For all devices, the time resolution FWHM is about 35 ps. Control and RCE SPAD with INV layer show clean exponential diffusion tails [7] with similar lifetimes (280 and 330 ps, respectively), whereas RCE SPAD with ACC layer show a second exponential component in the diffusion tail, with a lifetime of 2.6 ns.

According to Fig. 3, RCE SPAD with INV layer has a neutral region bounded at the top and bottom sides by depletion regions. As shown in [4], the diffusion tail is well described by a simple exponential law with a lifetime $\tau_d = w^2/(\pi^2 \cdot D_n)$, where w is the width of the neutral layer and D_n is the minority carrier (electron) diffusion coefficient.

Conversely, in RCE SPAD with ACC layer, the neutral region is bounded at the bottom side by the accumulated Si–SiO_2 interface. As a consequence: 1) the neutral region width w^* is larger than w and, 2) photogenerated electrons can make a double pass through the neutral zone after being backscattered at the buried interface. Based on simple symmetry arguments, we concluded that the slow component of the diffusion tail can be still modeled with a simple exponential decay with lifetime $\tau_d = (2w^*)^2/(\pi^2 \cdot D_n)$. Widths w and w^* were estimated by fitting experimental data with $D_n = 20$ cm^2/s, obtaining 2.6 and 3.5 μm, respectively.

IV. Conclusion

We presented the first RCE SPAD detectors with a buried DBR fabricated by means of a commercially reproducible double-SOI technique. RCE SPADs have peak photon detection efficiencies ranging from 42% at 780 nm to 34% at 850 nm along with excellent time resolution of 35-ps FWHM. Despite the higher defectivity of double-SOI substrates, 20-μm-diameter SPAD detectors exhibit a fairly low DCR of 3500 c/s at room temperature and a good yield. These detectors are suitable for demanding photon counting applications where both high PDE and picosecond time resolution are required.

References

[1] M. Ghioni, A. Gulinatti, I. Rech, F. Zappa, and S. Cova, "Progress in silicon single-photon avalanche diodes," *IEEE J. Sel. Topics Quantum Electron.*, vol. 13, no. 4, pp. 852–862, Jul./Aug. 2007.

[2] K. J. Gordon, V. Fernandez, P. D. Townsend, and G. S. Buller, "A short wavelength gigahertz clocked fiber-optic quantum key distribution system," *IEEE J. Quantum Electron.*, vol. 40, no. 7, pp. 900–908, Jul. 2004.

[3] V. Ntziachristos, J. Ripoll, L. V. Wang, and R. Weissleder, "Looking and listening to light: The evolution of whole-body photonic imaging," *Nature Biotechnol.*, vol. 23, no. 3, pp. 313–320, Mar. 2005.

[4] A. Spinelli and A. Lacaita, "Physics and numerical simulation of single photon avalanche diodes," *IEEE Trans. Electron Devices*, vol. 44, no. 11, pp. 1931–1943, Nov. 1997.

[5] M. S. Ünlü and S. Strite, "Resonant cavity enhanced photonic devices," *J. Appl. Phys.*, vol. 78, no. 2, p. 607, Jul. 15, 1995.

[6] M. K. Emsley, O. Dosunmu, and M. S. Ünlü, "Silicon substrates with buried distributed Bragg reflectors for resonant cavity-enhanced optoelectronics," *IEEE J. Sel. Topics Quantum Electron.*, vol. 8, no. 4, pp. 948–955, Jul. 2002.

[7] A. Lacaita, M. Ghioni, and S. Cova, "Double epitaxy improves single-photon avalanche diode performance," *Electron. Lett.*, vol. 25, no. 13, pp. 841–843, Jun 1989.